Journal of Experimental Botany, Vol. 63, No. 14, pp. 5259–5274, 2012
doi:10.1093/jxb/ers185 Advance Access publication 1 August, 2012
This paper is available online free of all access charges (see http://jxb.oxfordjournals.org/open_access.html for further details)

Journal of Experimental Botany
www.jxb.oxfordjournals.org

RESEARCH PAPER

Cell survival after UV radiation stress in the unicellular chlorophyte *Dunaliella tertiolecta* is mediated by DNA repair and MAPK phosphorylation

Candela García-Gómez*, María L. Parages, Carlos Jiménez, Armando Palma, M. Teresa Mata and María Segovia*

Department of Ecology. Faculty of Sciences. University of Málaga, E-29071, Spain
* To whom correspondence should be addressed. E-mail: candelagg@uma.es or segovia@uma.es

Received 22 March 2012; Revised 24 May 2012; Accepted 25 May 2012

Abstract

Ultraviolet radiation (UVR) induces damage in a variety of organisms, and cells may adapt by developing repair or tolerance mechanisms to counteract such damage; otherwise, the cellular fate is cell death. Here, the effect of UVR-induced cell damage and the associated signalling and repair mechanisms by which cells are able to survive was studied in *Dunaliella tertiolecta*. UVR did not cause cell death, as shown by the absence of SYTOX Green-positive labelling cells. Ultrastructure analysis by transmission electron microscopy demonstrated that the cells were alive but were subjected to morphological changes such as starch accumulation, chromatin disaggregation, and chloroplast degradation. This behaviour paralleled a decrease in F_v/F_m and the formation of cyclobutane–pyrimidine dimers, showing a 10-fold increase at the end of the time course. There was a high accumulation of the repressor of transcriptional gene silencing (ROS1), as well as the cell proliferation nuclear antigen (PCNA) in UVR-treated cells, revealing activation of DNA repair mechanisms. The degree of phosphorylation of c-Jun N-terminal kinase (JNK) and p38-like mitogen-activated protein kinases was higher in UVR-exposed cells; however, the opposite occurred with the phosphorylated extracellular signal-regulated kinase (ERK). This confirmed that both JNK and p38 need to be phosphorylated to trigger the stress response, as well as the fact that cell division is arrested when an ERK is dephosphorylated. In parallel, both DEVDase and WEHDase caspase-like enzymatic activities were active even though the cells were not dead, suggesting that these proteases must be considered within a wider frame of stress proteins, rather than specifically being involved in cell death in these organisms.

Key words: caspase-like enzymes, *Dunaliella tertiolecta*, cell death, cell survival, cellular proliferation nuclear antigen, cyclobutane–pyrimidine photodimers, DNA damage and repair, repressor of transcriptional gene silencing (ROS1), mitogen-activated protein kinases, ultraviolet radiation.

Introduction

Research on the environmental effects of UV radiation (UVR) in aquatic and terrestrial ecosystems has been widely fostered since the discovery of the ozone layer depletion over Antarctica, namely the 'ozone hole'. Such research was initially focused on UVB radiation (280–315 nm). However, it soon became known that many of the effects of solar UVR were also caused

Abbreviations: AMC, 7-amino-4-methyl coumarin; BER, base excision repair; CL, caspase-like; CPD, cyclobutane–pyrimidine dimer; DEVD, acetyl-l-aspartyl-l-glutamyl-l-valyl-l-aspartic acid-AMC DML, DEMETER-LIKE; ERK, extracellular signal-regulated kinase; JNK, c-Jun N-terminal kinase; MAPK, mitogen activated protein kinase; NER, nucleotide excision repair; PAR, photosynthetic active radiation; PCNA, cell proliferation nuclear antigen; PSII , photosystem II; ROS1, repressor of transcriptional gene silencing; Rubisco, ribulose-1,5-bisphosphate carboxylase/oxygenase; SD, standard deviation; TEM, transmission electron microscopy; UVR, ultraviolet radiation; WEHD, acetyl-l-tryptophyl-l-glutamyl-l-histidyl-l-aspartic acid α-(4-methyl-coumaryl-7-amide).

by wavelengths corresponding to the UVA range (315–400 nm) that were not affected by fluctuations in the stratospheric ozone. Therefore, it was obvious that natural levels of incident UVR (i.e. in the absence of ozone reduction) were enough to cause significant negative effects on the biota.

The deleterious effects of UVR on aquatic systems are due mainly to the decrease in the carbon uptake capacity of primary producers and to DNA damage. Aquatic ecosystems absorb a similar amount of atmospheric carbon dioxide as terrestrial ecosystems and produce half of the biomass of our planet. Both UVA and UVB reduce carbon incorporation rates of marine phytoplankton by modifying photosystem II (PSII) efficiency or the ribulose-1,5-bisphosphate carboxylase/oxygenase (Rubisco) pool (Häder *et al.*, 2007). A reduction in the performance of these targets decreases the ability of the cells to photosynthesize, thereby hampering the carboxylation process (Raven, 2011). In addition, UVR effects on DNA include the generation of several photoproducts that affect replication and transcription of the DNA, causing mutations and/or cell death (Lo *et al.*, 2005). The two major classes of mutagenic DNA lesions induced by UVR are cyclobutane–pyrimidine photodimers (CPDs) and the 6-4 photoproducts (6-4PPs) (Van de Poll *et al.*, 2002). UVR also stimulates base substitutions, as well as duplications and deletions in the DNA (Yoon *et al.*, 2000). CPDs such as TT, CC and TC dimers may arrest cell-cycle progression by inhibiting cell division due to the obstruction of *de novo* synthesis of cellular components required for cell growth and maintenance. DNA damage caused by exposure to UVR also induces the production of reactive oxygen species, which are one of the primary causes of DNA degradation in most aquatic organisms (Lesser, 2006). Consequently, growth is reduced or even arrested, driving the whole population into massive death, as described previously for natural phytoplankton communities (Llabrés and Agustí, 2006). Survival of the cells is based on the balance between damage induction rate and damage removal rate. Damage will accumulate when the capacity of the repair mechanisms is overloaded and is not sufficient to reverse the harmful effects induced/caused by UVR. Therefore, repair of oxidative and mutagenic DNA lesions is essential to prevent mutations and cell death (Roldán-Arjona *et al.*, 2000; Morales-Ruiz *et al.*, 2006; Ponferrada-Marín *et al.*, 2010).

Considerable evidence has been accrued to demonstrate that when cells are stimulated by biotic or abiotic stress, a complex network of specific protein phosphorylations and dephosphorylations takes place [by the so-called mitogen-activated protein kinases (MAPKs)], leading to the activation and/or de-activation of specific group of genes (Kyriakis and Avruch, 2001). This process generally leads to a response that allows the cell either to adapt to the new conditions or to enter into a process that will end up in cell death. MAPKs are grouped in canonic tri-modules, and three of these cascades—extracellular signal-regulated kinase (ERK), c-Jun N-terminal kinase (JNK) and p38—have been described completely in mammalian cells. Recent studies indicate that MAPK signalling cascades are also present in vascular plants such as *Arabidopsis*, *Nicotiana* and *Oryza* (Nakagami *et al.*, 2005). However, while the above-mentioned three MAPK subfamilies (ERK, JNK and p38) are present in animal cells, plant kinase genes appear to belong solely to the ERK subfamily (Zhang *et al.*, 2006). The presence of MAPK-like pathway components in algae has been described previously by our group (Jiménez *et al.*, 2004, 2007). We reported the presence of both p38- and JNK-like MAPKs in *Dunaliella viridis* and their involvement in survival of hyperosmotically stressed cells, demonstrating the presence of ERK1/2 in this microalga and its participation in cell division, including a partial cloning of both MAPKs. Very recently, the expression of MAPK-like proteins in response to stress has been also shown in intertidal macroalgae (Parages *et al.*, 2012). Taken together, these results indicate that algae possess MAPK-like signalling components that serve to sense and respond to stress, permitting cell acclimation and survival under the new conditions.

Thus, cells have different DNA repair mechanisms to counteract the lethal effects of abiotic injuries, allowing them to maintain their genetic integrity. The most important repair mechanisms are photoreactivation and excision repair. During photoreactivation, the enzyme photolyase in combination with photorepair wavelengths between 330 nm and visible light are able to reverse the UVB-induced production of CPDs. Photolyase binds to CPDs in the DNA and, after absorbing a near-UV or blue light photon, it splits the cyclobutane ring to restore the pyrimidine. The photoreactivation process has been demonstrated widely in phytoplankton (Boelen *et al.*, 2001; Yi *et al.*, 2006), and in the particular case of *Dunaliella tertiolecta* we have cloned a CPD photolyase expressed in this species (García-Gómez C, Cano I, Mata MT and Segovia M. GenBank accession no. JF260981) under chronic UVR exposure. In contrast, excision repair mechanisms are able to replace either the damaged base [base excision repair (BER)] or the whole damaged nucleotide [nucleotide excision repair (NER)] in the DNA. During BER, different DNA *N*-glycosylases cleave the glycosylic bond between the target base and deoxyribose (García-Ortiz *et al.*, 2001; Roldán-Arjona and Ariza, 2009), whilst during NER, the gap formed is replaced by DNA polymerases.

The cell proliferation nuclear antigen (PCNA) is an auxiliary protein of the δ/ε DNA polymerase, which is essential for DNA synthesis. Its synthesis and abundance is cell-cycle dependent and it increases during the S phase. PCNA is generally expressed, and the protein accumulated in phytoplankton under normal growth conditions, indicating cell proliferation (Carpenter *et al.*, 1998). However, previous reports have shown compelling evidence that PCNA is also expressed and the protein accumulates at high rates in cells exposed to UVR, evidencing its participation during DNA repair by both BER and NER pathways (Masih *et al*., 2008). A second nuclear protein, the repressor of transcriptional gene silencing (ROS1), also participates in UVR-induced repair mechanisms. This protein was studied for its role in epigenetic control of gene expression (Gong *et al.*, 2002), but it contains an endonuclease III domain with significant similarities to BER DNA proteins in the HhH-GPD superfamily (Ponferrada-Marín *et al.*, 2010). Such family contains a diverse range of structurally related DNA repair proteins including endonuclease III [DNA glycosylase/apurinic/apyrimidinic (AP) lyase] and MutY (A/G-specific adenine glycosylase) (Krokan *et al.*, 1997; Scharer and Jiricny, 2001). The genome of *Arabidopsis* encodes several other proteins belonging to the HhH family of DNA glycosylases, all with similar DNA repair activities to homologues found in bacteria, fungi and animals (Roldán-Arjona *et al.*, 2000;

García-Ortiz *et al.*, 2001). All these proteins act as DNA glycosylases, removing oxidized pyrimidines from the DNA, as well as AP lyase, by cleaving the phosphodiester back-bone by β-elimination at the site where a damaged base has been removed. In addition, genetic and biochemical studies have revealed that the *Arabidopsis* protein ROS1, which contains a DNA glycosylase domain, initiates the deletion of 5-methylcytosine though a BER process (Ortega-Galisteo *et al.*, 2008).

UVR is usually considered to be a stressor for phytoplankton that reduces the photosynthetic uptake of atmospheric carbon dioxide and affects species diversity, ecosystem stability, trophic interactions and global biogeochemical cycles, driving microalgae into decreased cell viability and, in most of species, leading to cell death. The occurrence of programmed cell death (PCD) as an active mechanism by which mass cell death takes place as a consequence of biotic and abiotic stress has been widely reported in unicellular chlorophytes (Segovia *et al.*, 2003; Darehshouri *et al.*, 2008; Zuppini *et al.*, 2010), dinoflagellates (Vardi *et al.*, 1999; Bouchard and Purdie, 2011), cyanobacteria (Ross and Paul, 2006), diatoms (Timmermans *et al.*, 2007), haptophytes (Bidle *et al.*, 2007; Franklin *et al.*, 2012), and natural communities (Veldhuis *et al.*, 2001). The mechanisms by which cell death (programmed or not) occurs, considering that cell death in unicells leads to the complete demise of the organism, are always intriguing and there are still many unanswered questions (Nedelcu *et al.*, 2011). Among these are the questions of what is the proteolytic machinery involved and how it works. Caspase-like (CL) activities have been reported to be involved in PCD in plants, fungi, protists, and protozoa (Bonneau *et al.*, 2008; Pérez-Martín, 2008). Regarding phytoplankton, the nature of CL activities remains an unrevealed question. Although it is known that CL activities are involved in cell death, these proteases are also essential during the normal physiology of the cells with constitutive functions, as well as during growth and cell stress acclimation (Segovia and Berges, 2005; Bouchard and Purdie, 2011).

Microalgae from the genus *Dunaliella* are among the most ubiquitous eukaryotic organisms and are well known for their extraordinarily high tolerance to salinity, temperature, nutrient limitation, and irradiance (Ben-Amotz *et al.*, 2009). These features make these microalgae perfect candidates as model organisms for the study of environmental stress responses. As such, in previous works, we have shown that survival of the halotolerant species *D. viridis* subjected to environmental stress was crucially dependent on phosphorylation of p38- and JNK-like MAPKs. Cell division was impaired after hyperosmotic shock, UVR, heat shock, and nutrient starvation, caused by a marked decrease in the phosphorylated form of ERK. However, depending on the stress factor and on its intensity, cells underwent PCD, as demonstrated morphologically and by an increase in the CL activity DEVDase (Jiménez *et al.*, 2004, 2007, 2009).

The aim of this work was to elucidate why *D. tertiolecta* cells did not die when subjected to chronic UVR exposure and the reasons for their resistance. For this purpose, we studied the dynamics of DNA damage accumulation and repair, with regard to cell death and/or survival. We showed that cells survived chronic UVR exposure by activation of DNA repair mechanisms by means of PCNA and ROS1-protein accumulation. Concurrently, we demonstrate that activation of MAPK-like proteins mediated the process and we have also provided evidences that CL proteins, mainly regarded as cell death proteases, are also involved in the response to stress. As such, these proteases must be considered within a wider frame of stress proteins, rather than being specifically involved in cell death in these organisms.

Materials and methods

Culture conditions

The unicellular chlorophyte *D. tertiolecta* (CCAP 19/6) was used in this work. Cells were grown in sterile acrylic cylinders (Plexiglas XT® 29080) transparent to UV, in artificial seawater (Goldman and McCarthy, 1978) f/2 enriched (Guillard and Ryther, 1962). The cells were maintained at 16 ºC, under continuous stirring and bubbling, at an irradiance of 100 µmol quanta m^{-2} s^{-1}, until they reached mid-exponential growth phase, when treatment was begun. The treatments comprised the application of photosynthetically active radiation (PAR) or PAR+UVA+UVB. The different irradiance conditions where achieved by covering the experimental cylinders with cut-off filters. Ultraphan UBT 395 (Digefra, München, Germany) transmitted only PAR (P treatment), while Ultraphan UBT 295 (Digefra, München, Germany) transmitted PAR, UVA and UVB (PAB treatment). PAR was obtained by using Optimarc 250 W lamps (DuroTest, USA) and measured using an Ocean Optics SMS 500 spectroradiometer (Sphaereoptics, Contoocook, New Hampshire, USA) calibrated after *National Physical Laboratory* standards with a cosine-corrected sensor. UV fluence rates were provided by Qpanel-340 lamps (9.5 Wm^{-2} UVA and 0.45 Wm^{-2} UVB, unweighted) and measured with a MACAM UV203 radiometer (MACAM Photometrics, Livingston, UK) and with the Ocean Optics SMS 500 spectroradiometer mentioned above. Spectra were measured in the range 250–800 nm. All light measurements were carried out inside the cylinders once they were wrapped with the appropriate cut-off filters.

Cell abundance and cell death

For cell counts, 1 ml of fresh cell culture was counted in a Coulter Counter (Z2 Beckman Coulter, Fullerton, CA, USA). The growth rate (r) was calculated as the number of cell doublings day^{-1} by fitting an exponential function to the logarithmic phase of the growth curve. Cell death was estimated using SYTOX Green (Invitrogen, OR, USA) according to the method of Segovia and Berges (2009). Basically, cell pellets were resuspended in 1 ml of 10 mM PBS buffer (pH 7) containing SYTOX Green at a final concentration of 20 µM, incubated at 16 °C in the dark for 30 min and analysed by flow cytometry using a DakoCytomation flow cytometer (MoFlo, Beckman Coulter, Fullerton, CA, USA) and under an epifluorescence microscope (Leitz, Wetzlar, Germany) at an excitation wavelength of 450–490 nm and emission wavelength of 523 nm. Positive controls consisted of cells killed by fixation with 1% glutaraldehyde. Samples were analysed in triplicate.

In vivo *chlorophyll a fluorescence*

The optimal quantum yield of PSII fluorescence (F_v/F_m) was measured with a Water-PAM fluorometer (Waltz, Effeltrich, Germany) as described by Schreiber *et al*. (1986), considering F_v/F_m as $(F_m - F_o)/F_m$ according to Genty *et al*. (1989), F_v is the maximal variable fluorescence of a dark-adapted sample, F_m is the maximal fluorescence intensity with all PSII reaction centres closed, and F_o is the basal fluorescence. High F_v/F_m values indicate that cells are in a good condition, whereas a decrease in F_v/F_m indicates stress and photoinhibition.

Flow cytometry

DAPI is a popular nuclear counter-stain for use in multicolour fluorescent techniques. Its blue fluorescence stands out in vivid contrast to the green,

yellow, or red fluorescent probes of other structures and it specifically stains nuclei, with little or no cytoplasmic labelling. DAPI (Molecular Probes, Eugene, OR, USA) was added at a concentration of 1–10 µM and incubated for 5 min at room temperature according to the method of Jiménez et al. (2009). Samples were analysed using a DakoCytomation flow cytometer. Counts were triggered using forward scatter signals. DAPI fluorescence was observed through a 435–485 nm band-pass filter and chlorophyll fluorescence through a 650–710 nm band-pass filter.

Transmission electron microscopy (TEM)

Cells were harvested by centrifugation (15 min at 7000 *g*) and fixed in cacodylate buffer (100 mM, pH 7.2) containing 4% glutaraldehyde and 8.6 % sucrose. Pellets were washed in a series of cacodylate buffers with descending sucrose concentration and post-fixed in 1% osmium tetroxide dissolved in Milli-Q ultrapure water (Millipore, USA) for 2 h. After dehydration in an ascending series of ethanol (70–100%), samples were embedded in 4 % agar resin and ultrathin sections (60 nm thickness) were prepared with a Reichert-Jung ultramicrotome (Leipzig, Germany). Sections were stained with uranyl acetate and lead citrate, and observed under a Philips CM 100 transmission electron microscope at different magnifications. Quantification of cells by TEM can be problematic; therefore, counting of cells showing each of the different characteristics was carried out for three fields of view for each treatment at the lowest magnification.

DNA damage

For the detection of DNA damage, 25 ml of *D. tertiolecta* was collected by centrifugation and the pellets frozen at –80° C. DNA was extracted following the procedure provided with the DNeasy Plant Mini kit (Qiagen, VA, USA). The extracted DNA was quantified using the fluorescent probe Quant-iTTM PicoGreen® kit (Invitrogen, OR, USA,) and CPDs were analysed by a modification of the protocol described by Boelen et al. (1999). Thirty nanograms of DNA in 200 ml of TE buffer [10 mM Tris/HCl (pH 7.5), 1 mM EDTA final concentration] were loaded onto a nylon HybondTM-N+ membrane. The membrane was incubated overnight at 4 °C with a primary anti-thymine dimer H3 monoclonal antibody (Affitech, Oslo, Norway) (diluted 1:600). After the appropriate washes and incubation with horseradish peroxidase-conjugated anti-mouse secondary antibody (diluted 1:5000) (Abcam, Cambridge, UK), the signal was detected by chemiluminescence (ECL; GE Healthcare, Buckinghamshire, UK) and the intensity of cross-reactions was quantified using a Gel Logic Image Analyser (Eastman-Kodak, Rochester, NY, USA).

Western blots

PCNA and ROS1

For PCNA and ROS1 detection and protein accumulation studies, SDS-PAGE (12 % acrylamide) was performed on an equal protein concentration basis. Proteins were extracted according to the method of Segovia and Berges (2005). For PCNA immunodetection, blots were probed with anti-PCNA-at263 antibody at a 1:2000 dilution (Santa Cruz Biotechnology, California, USA). For ROS1 immunodetection, blots were probed with an anti-*Arabidopsis thaliana* ROS1 protein polyclonal antibody (α-AtROS1) kindly provided by Professor Teresa Roldán-Arjona (Córdoba University, Spain; Gong *et al.*, 2002; Morales-Ruiz *et al.*, 2006) at a 1:1000 dilution. An antigenic AtROS1 Sepharose-purified recombinant protein was also used as the antibody-blocking peptide (blockage binding-site ratio of 1:4, antibody:recombinant protein, in moles) to check for absolute specificity of the antibody, as well as for positive controls. Antibodies were also blocked with Rubisco to ensure that there was no recognition of this protein, as we were using an anti-rabbit polyclonal antibody. Pre-immune sera were used for the appropriate non-specific ROS1-reactivity negative controls. Additionally, a secondary antibody non-specific cross-reactivity control was carried out by incubating the membranes with the secondary antibody only in absence of the primary antibody.

ERK, p38, and JNK kinases

For MAPK extraction, 15 ml of *D. tertiolecta* culture of each treatment were centrifuged in duplicates (1500 *g*, 10 min) at room temperature. Pellets were resuspended in 100 µl of 10 % SDS, and gently mixed with 400 µl of MAPK lysis buffer [50 mM β-glycerophosphate (pH 7.2), 0.1 mM sodium vanadate, 2 mM $MgCl_2$, 1 mM EGTA, 1 mM dithiothreitol, 2 µg ml^{-1} leupeptin, 4 µg ml^{-1} aprotinin]. Samples were placed in a pre-cooled sonicating water bath (Branson 2510; Branson Ultrasonic Corp., Danbury, CT, USA) for 5 min. A centrifugation step (4° C, 30 min, 15 000 *g*) was applied to remove all cell debris and the supernatant was assayed for protein quantification by the BCA method. Western blots were performed by modifying the protocol described previously by Jiménez et al. (2004), in which tricine was used instead of glycine in the gels for better resolution. Antibodies against the phosphorylated forms of p38, JNK, and ERK MAPKs, as well as their specific blocking peptides, were purchased from Cell Signaling Technology (Beverly, MA, USA). The possibility of non-specific cross-reactivity with the antibodies raised against the phosphorylated forms of the MAPKs from mammalian cells was also analysed by incubating at least one lane of each treatment directly with the secondary antibodies, avoiding contact with the primary ones. Non-specific bands were not included in further analyses. The signal on the membranes was detected by chemiluminescence, as described above.

CL activities

Cells were harvested by centrifugation and resuspended in lysis buffer [50 mM HEPES (pH 7.3), 100 mM NaCl, 10 % sucrose, 0.1 % CHAPS, 10 mM dithiothreitol] and sonicated (UP50H; Hielscher GmbH, Germany) on ice. Extracts were mixed with 50 µM (final concentration) of 7-amino-4-methyl coumarin (AMC) of the labelled substrates acetyl-L-tryptophyl-L-glutamyl-L-histidyl-L-aspartic acid-AMC (WEHD) and acetyl-L-aspartyl-L-glutamyl-L-valyl-L-aspartic acid-AMC (DEVD) (Peptanova GmbH, Germany). The fluorescence emitted as a consequence of substrate cleavage was measured for 4 h at 16 °C (excitation 360 nm, emission 460 nm) in a microplate fluorescence reader (FL-600; Bio-Tek, Vermont, USA), according to the method of Segovia and Berges (2005).

Statistical analysis

Data were checked for heterogeneity of variances and for normality using Cochran and Mann–Whitney' U tests, respectively. Differences due to the effect of light treatments and time were then tested by two-way analysis of variance (ANOVA) and ANOVA-RM. Where significant differences were detected, post-hoc multiple comparisons were applied using Holm-Sidak or Newman–Keuls tests (considering $P < 0.05$ as significant). To quantify the relationship between the variables, we performed Pearson's product-moment correlations (considering $P < 0.05$ as significant). Values are expressed as means ±standard deviation (SD). The statistical analyses were carried out using the SigmaPlot 11.0 statistical package (SPSS Inc., Chicago, IL, USA).

Results

Cell abundance and cell death

The cell density of *D. tertiolecta* (Fig. 1A) increased in P treatment during the time course of the experiment, reaching the stationary phase at 144 h, by which time the cell cultures had started to decay ($r = 0.44$ dd^{-1}). Unexpectedly, we observed a net growth in UV-exposed cultures, although the cell density increase was nearly four times lower under PAB than under P treatment ($r = 0.12$ dd^{-1}).

Cell death was checked with the fluorescent probe SYTOX Green. When the plasma membrane is compromised, cells incubated with this nucleic acid stain will fluoresce green, whereas

living cells appear red due to the autofluorescence of chlorophyll *a*. Over the time course of the experiments, approximately 99% of the cells were alive and swimming in both treatments, as demonstrated by the absence of green fluorescent labelling and by the presence of chlorophyll red fluorescence (Fig. 1A, insert). The presence of green fluorescence in the positive control corresponding to dead cells killed by fixation with glutaraldehyde (data not shown) confirmed the integrity of the cells in all treatments. Hence, cell death was not detected in any of the cultures stressed with UVR.

Photosynthetic efficiency

The optimum quantum yield of PSII (F_v/F_m) was used as an indicator of stress and photoinhibition (Fig. 1B). The F_v/F_m value dropped significantly from values close to 0.6 at the beginning of the experiments to values below 0.09 in just 2 h under UVRtreatment (data not shown) and to 0.2 in 24 h. The values with P treatment were significantly different throughout the experiment and were about 6-fold higher than under PAB treatment. UVR-exposed cells were transferred to a recovery treatment under P conditions to contrast the results obtained with SYTOX Green, indicating the absence of cell death. Under these conditions, the F_v/F_m value showed an increase of 200% from the minimum value in only 24 h under P treatment, and these values were maintained until 72 h.

Cell cycle

The results obtained for F_v/F_m were confirmed by flow cytometry analysis. Flow cytometry (Fig. 2A) showed that when cultures

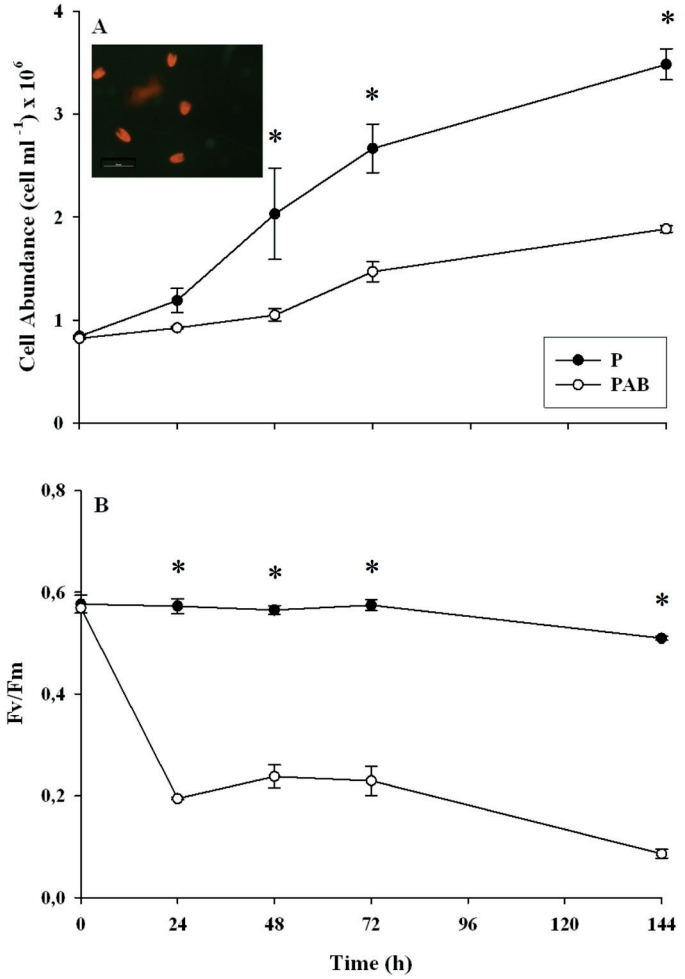

Fig. 1. (A) *D. tertiolecta* cell abundance in cultures grown under continuous P (closed symbols) or continuous PAB (open symbols) conditions. (B) Changes in the optimum quantum yield (F_v/F_m) in cultures grown under P (closed symbols) or PAB (open symbols) conditions. Symbols are the mean ±SD of two replicates. The insert shows a representative epifluorescence micrograph of SYTOX Green-treated cells. The chlorophyll red fluorescence in cultures grown under PAB treatment demonstrates that the cells are alive. Statistically significant differences (P <0.05) between treatments are indicated by asterisks.

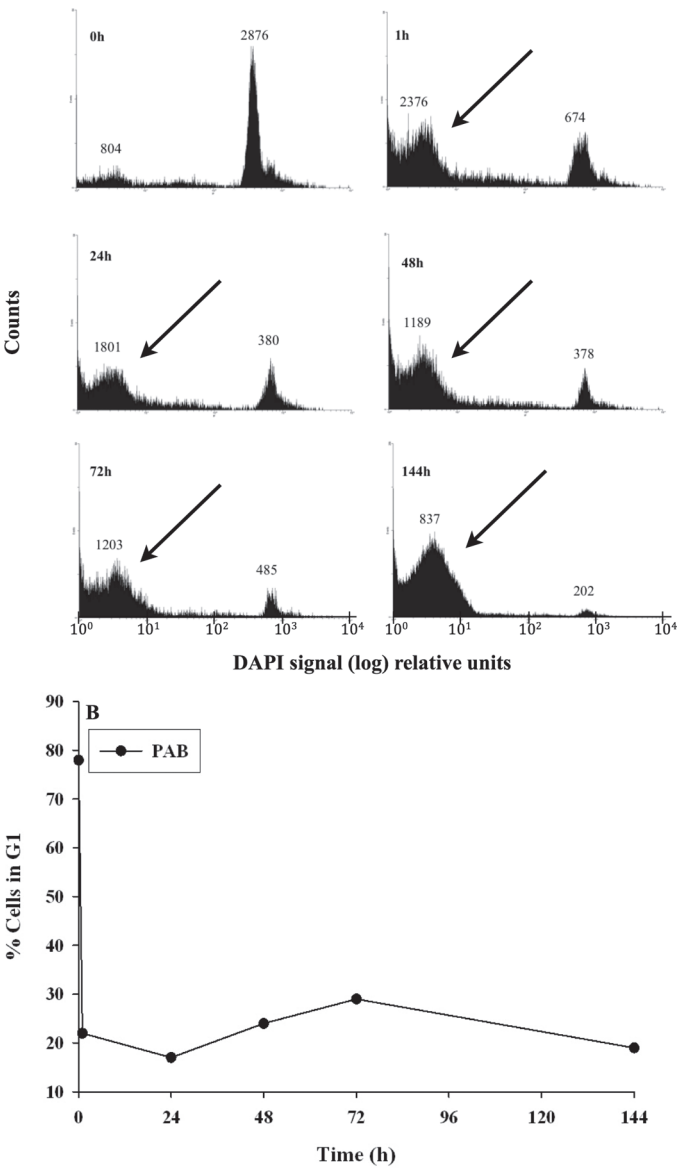

Fig. 2. (A) Flow cytometry analysis of DAPI-labelled *D. tertiolecta* cells exposed to PAB. (B) Variation in the number of cells in the G1 phase of the cell cycle with respect to the total number of cells counted during PAB treatment.

were in the mid-exponential phase (t = 0 before UVR exposure), 78 % of the cells were in the G1 phase of the cell cycle (Fig. 2B). However, only after 1 h of PAB treatment, the number of cells in G1 decreased dramatically to 22 %, and this value did not change significantly during the rest of the experiment, with no parallel increase in counts in other stages of the cell cycle. However, there was a significant increase in DAPI fluorescence (Fig. 2A, arrows), indicating chromatin disaggregation, without indicating any shift in the chromatin content as a result of the cell cycle.

Cell morphology

The cell cycle results paralleled the cell morphology observed by TEM (Fig. 3). Micrographs showed normal vegetative cells growing under PAR conditions, with conspicuous Golgi, mitochondria, chloroplasts, pyrenoids, and scarce starch spots. Nuclei were well defined and surrounded by the nuclear membrane, with the chromatin compacted in the nucleoli. From 72 h onwards, cells presented symptoms of senescence, and by the end of the experiment, most of the cells showed chromatin marginalization (144 h) while the organelles remained intact. When cells were cultured under PAB conditions, their morphology was also unaltered, and the nucleolus was well structured in the nucleus; however, the chromatin started to disaggregate and formed dense spots at early stages of exposure, while the appearance of the organelles did not change. In addition, starch accumulation in the cytoplasm occurred from 48 h onwards, coincident with slight chloroplastic degradation. The micrographs did not provide evidence for cell death indicators under UVR exposure.

DNA damage and repair

The presence of CPDs is a direct indicator of DNA damage. The evident effect of UVR exposure on CPD accumulation can be seen in Fig. 4. Both P and PAB treatments presented a low intensity pattern for CPD accumulation at the initial time (t = 0), which was not significant ($P > 0.05$). During the course of the experiment with P treatment, CPD accumulation did not change significantly. However, cells exposed to UVR (PAB treatment) suffered a remarkable 5-fold increase by 24 h. From 72 h onwards, there was an increase in the intensity of the dots, peaking at 144 h. At this point, differences between the two light treatments were 7-fold higher under PAB treatment and more than 8-fold when compared with the initial values.

We studied two proteins directly related to DNA repair after UV stress, PCNA and ROS1. PCNA accumulated at a high rate in cells exposed to UVR, indicating its participation during both BER and NER pathways. Differences in PCNA accumulation during the two light treatments were estimated by the relative intensity of the immunologically detected 36 kDa band (Fig. 5A). PCNA trends were highly similar to the pattern obtained for CPD formation (Fig. 4). The results showed a basal amount of PCNA protein with P treatment that did not change significantly over the time course of the experiment ($P > 0.05$). However, when UVR was present, the PCNA level was slightly augmented at 24 h. Nevertheless, at 48 and 72 h its concentration increased 4 and 7-fold, respectively, compared with the P treatment and with the level at $t = 0$ before UVR exposure.

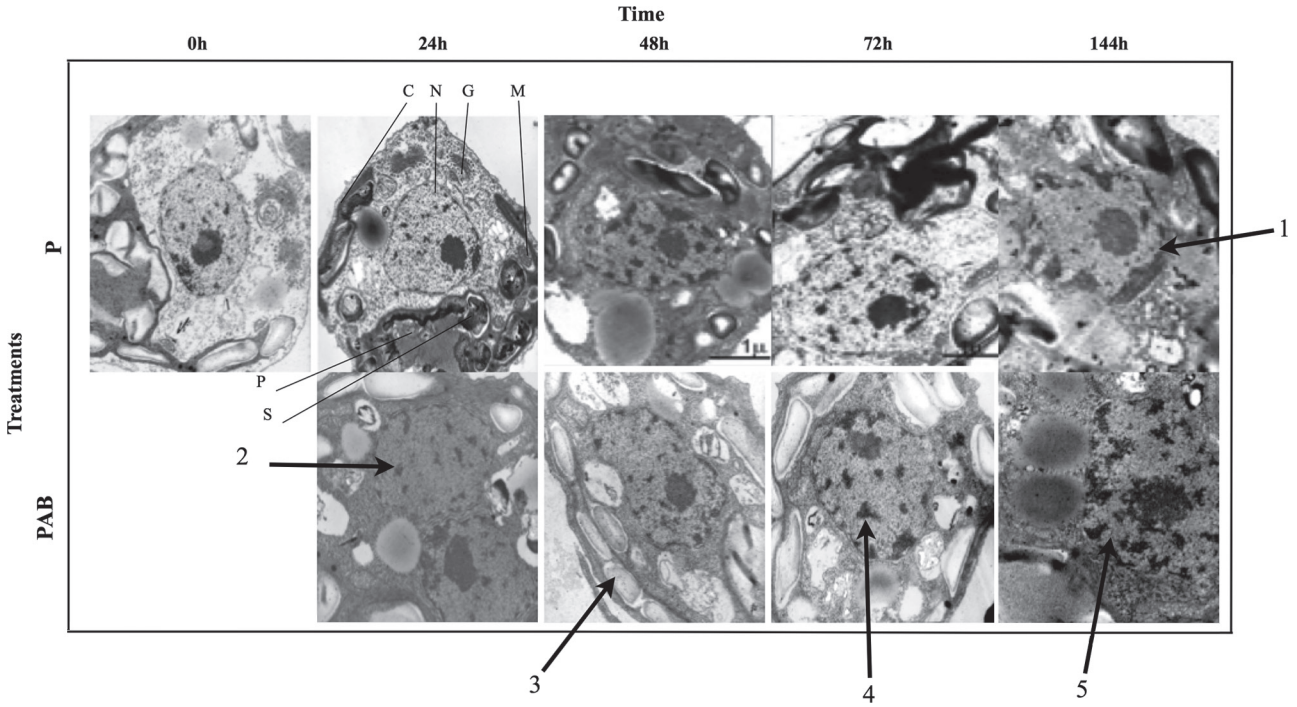

Fig. 3. Representative transmission electron micrographs showing the morphological changes in *D. tertiolecta* cultures exposed to P or PAB treatment. C, chloroplast; N, nucleus; G, Golgi, M, mitochondria; P, pyrenoid; S, starch. Note the chromatin marginalization (arrow 1) due to natural senescence of the cultures under P treatment, and the cellular changes associated with UVR exposure such as chromatin spots (arrows 2 and 4), starch accumulation and slight chloroplastic degradation (arrow 3), and chromatin disaggregation (arrow 5). Bar corresponds to 1 µm.

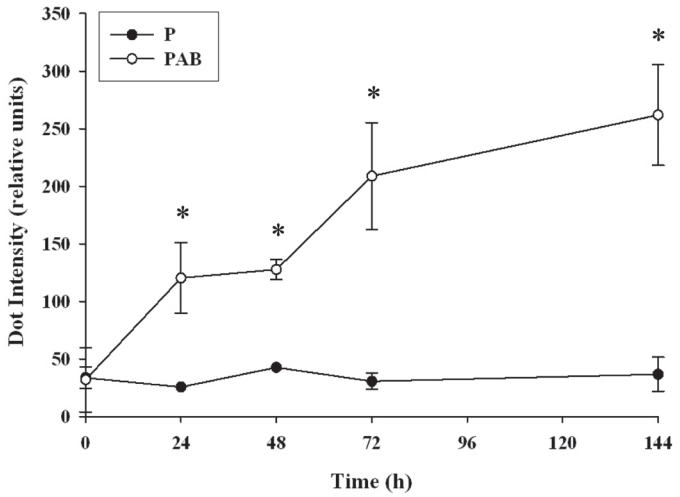

Fig. 4. Quantification of the intensity of the dots under P (closed symbols) or PAB (open symbols) treatments. Data points are the mean±SD of three replicates. Statistically significant differences ($P < 0.05$) between treatments are indicated by asterisks.

ROS1 also participates during repair mechanisms caused by UVR. It was found that the antibody against ROS1 from *A. thaliana* detected a 52 kDa band. As found for PCNA, with both the P and PAB treatments, *D. tertiolecta* presented a basal amount of ROS1 protein at the start of the experiment (t = 0). As before, in control cultures under P conditions, ROS1 levels did not change significantly during the course of the experiment. However, when cells were cultured under PAB, protein accumulation increased significantly after 48 h, reaching values three to six times higher than with P treatment after 72 h and 144 h, respectively (Fig. 5B). In order to ensure that the bands detected by the antibody corresponded to the recombinant ROS1 protein, the binding site between the protein and the primary antibody was specifically blocked as described in Materials and Methods. In the presence of the blocked antibody, a clear reduction in the intensity of the bands (>90%) was seen, confirming that detection was indeed specific for ROS1 protein (data not shown).

MAPK phosphorylation in response to stress

Phosphorylation of the JNK-like MAPK in *D. tertiolecta* under P and PAB treatment is depicted in Fig. 6A. It can be seen that a clear 45 kDa band was detected by the antibody against the phosphorylated form of mammalian JNKs. Basal phosphorylation of this JNK-like protein occurred before the light treatments (Fig. 6A, $t = 0$), indicating that constitutive phosphorylation of this MAPK-like protein exists in this microalga. In addition, a significant increase in phosphorylation occurred over the following 48 h with PAR treatment, coinciding with the time when cultures reached their loading capacity. At 144 h, during the stationary phase of growth, the degree of phosphorylation dropped off to initial levels. The pattern changed when UVR was applied to the cultures. The degree of phosphorylation was always higher under PAB than under P treatment after 48 h of culture. Maximum phosphorylation was found at 72 h, but a decrease to initial levels was not detected at 144 h, as was found with PAR treatment. To be sure that the bands detected by the specific phosphorylated JNK antibody corresponded to a JNK-like protein in *D. tertiolecta*, the binding site between the protein and the primary phospho-antibody was again specifically blocked by using specific blocking peptides as indicated in Materials and Methods. These peptides abolished the signals from the indicated phospho-JNK MAPK, confirming that the antibody was indeed specific for a phospho-JNK-like protein (data not shown).

Phosphorylation of a p38-like MAPK was also detected. The results presented in Fig. 6B show the different behaviour of phosphorylation after P or PAB treatment. Activation of a 40 kDa p38-like MAPK was very scarce under P conditions; however, a significant increase in phosphorylation was detected in the presence of UVR. It can be seen that the degree of phosphorylation peaked 24 h after the initiation of the light treatment (band intensity was 2.5 times higher than at $t = 0$ and than in control PAR cultures). This phosphorylation was reduced to initial levels over the following 48 h. The use of p38-specific blocking peptide also greatly reduced, almost to undetectable levels, the intensity of the band of this p38-like MAPK, indicating the high degree of similarity between this protein in *D. tertiolecta* and the mammalian p38. Finally, we tested the specific phospho-ERK1/2 antibodies of mammalian origin. It was clear that a 44 kDa ERK-like MAPK was activated by P treatment to much higher levels than by PAB treatment after 24 h (Fig. 6C). From this point, the degree of phosphorylation was reduced almost to initial levels after 144 h under P conditions. In contrast, the degree of phosphorylation showed small changes under PAB treatment over the course of the experiments. The use of a specific blocking peptide of mammalian ERK resulted in a total disappearance of the band, indicating that this protein is similar to a mammalian ERK1/2.

CL activities

Caspase-like activities were analysed to check whether these enzymes were present and/or active, even though the cells were not dead. DEVDase activities were found to be constant and lower than WEHDase activities, and did not experience any significant change during UVR exposure ($P > 0.05$) (Fig. 7). However, the pattern of DEVDase activity was different with P treatment, where the activity increased about 3-fold during the first 24 h compared with PAB treatment, and finally dropping off to initial values after 72 h (Fig. 7A). Under PAB treatment, no significant variation in DEVDase activity was found during the experiment. In contrast to DEVDase, WEHDase activity (Fig. 7B) initially increased under PAB treatment at 24 h, showing a fluctuating pattern around the initial values for the rest of the experiment. When UVR was not present (P treatment), the enzymatic activity decreased dramatically at about 7-fold. These results demonstrated that both pathways were active, showing a broad range of enzymatic activity depending on the treatments, even though the cells were not dead.

Discussion

Effects of UVR on cell death or survival, photosynthesis and cell morphology

When aquatic organisms are subjected to stressful irradiance, the most compelling sign of photosynthetic capacity loss due

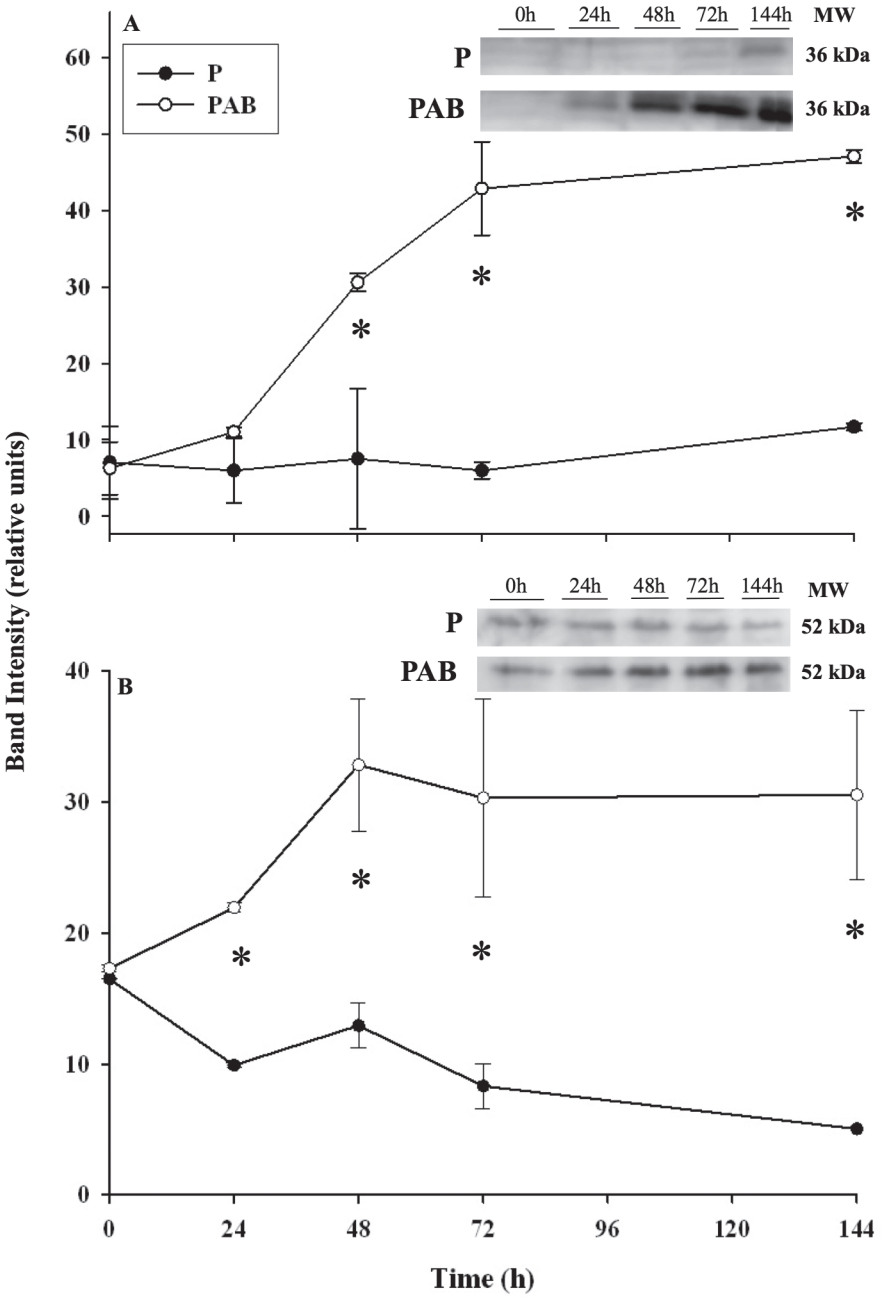

Fig. 5. Western blots showing cross-reactions of protein extracts from cultures of *D. tertiolecta* under continuous P (closed symbols) or continuous PAB (open symbols) with two *A. thaliana* polyclonal antibodies raised against PCNA (A), which showed a clear 36 kDa band, and ROS1 (B), which revealed a single band of 52 kDa. Results are shown as the mean±SD of two replicates. Statistically significant differences ($P < 0.05$) between treatments and bands obtained by image analyses are indicated by asterisks.

to photoinhibition is a sharp decrease in optimal quantum yield. When *D. tertiolecta* cells were exposed to PAB treatment, there was a dramatic decrease in F_v/F_m in just 2 h of exposure from 0.6 to 0.09. Several studies in algae have described the oxidative degradation of the D1 protein in the PSII reaction centre (Hanelt, 1998) after exposure to excess irradiance. Despite the initial decline in F_v/F_m in cultures under PAB treatment, the values obtained for this parameter indicated the presence of some photosynthetic activity and, consequently, that the cells were able to tolerate high UVR doses (Fig. 1B), probably due to DNA and other cellular component repair processes. The decline in F_v/F_m in PAB cultures was due to cell damage, as demonstrated by the morphological analysis showing degradation of the chloroplasts from 48 h onwards (Fig. 1B) and as also observed by Melis *et al*. (1992) and Bouchard *et al*. (2005). When UVR is added to PAR, DNA damage means that the synthesis of essential proteins does not occur (Jordan, 1996; Meador *et al.*, 2009). Thus, in addition to D1 and PSII reaction centre degradation, the electron transport chains and photophosphorylation processes are inhibited, and the electron-demanding Rubisco content also

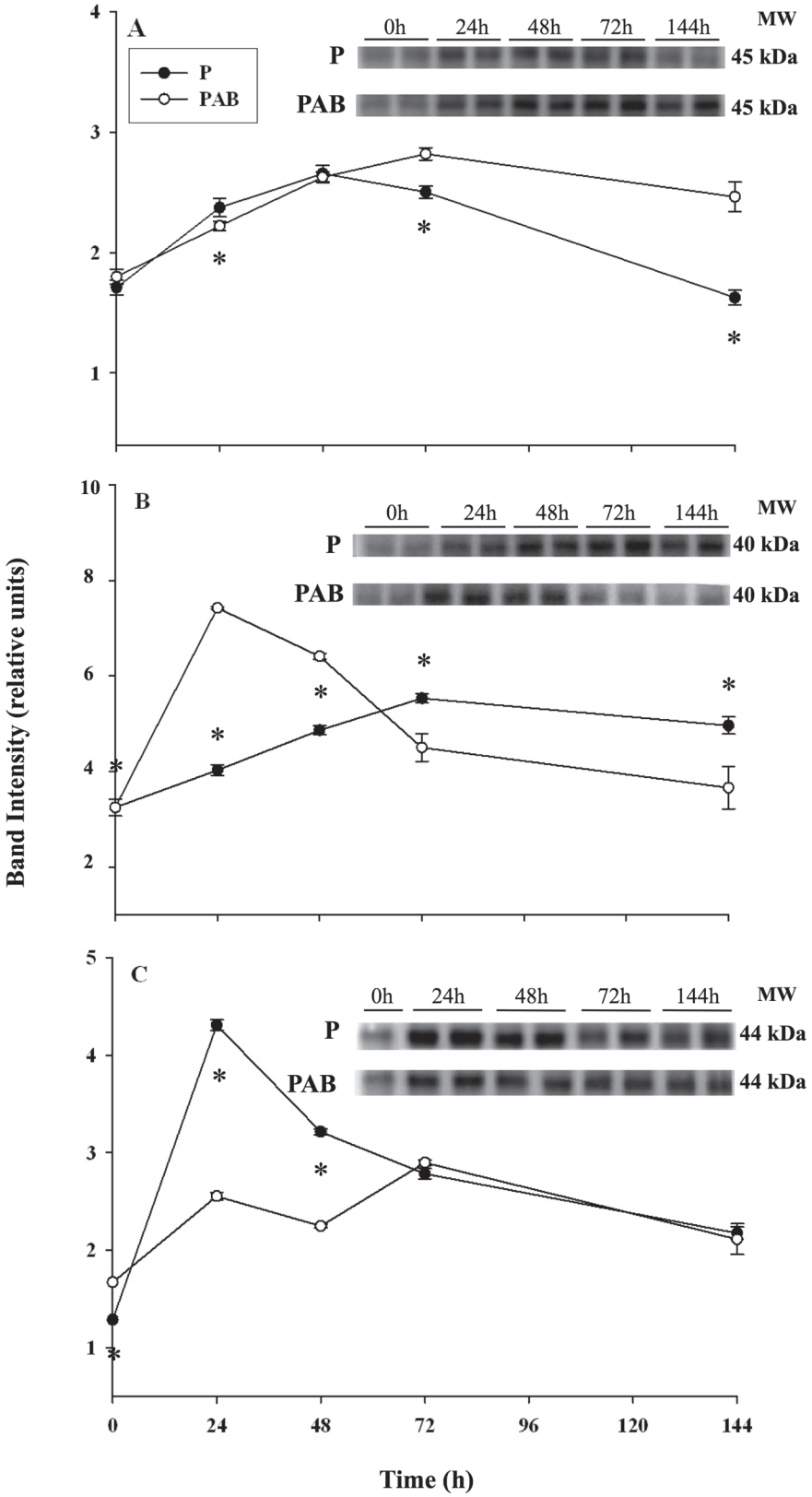

Fig. 6. Western blots showing the phosphorylated forms of MAPK-like proteins in *D. tertiolecta* under continuous P (closed symbols) or continuous PAB (open symbols) treatment using polyclonal antibodies raised against phosphorylated JNK (A), which revealed the presence of a single band of 45 kDa, phosphorylated p38 (B), which cross-reacted with a specific 40 kDa protein, and phosphorylated ERK (C), which showed a clear 44 kDa band. Statistically significant differences (P <0.05) between treatments and bands obtained by image analyses are indicated by asterisks.

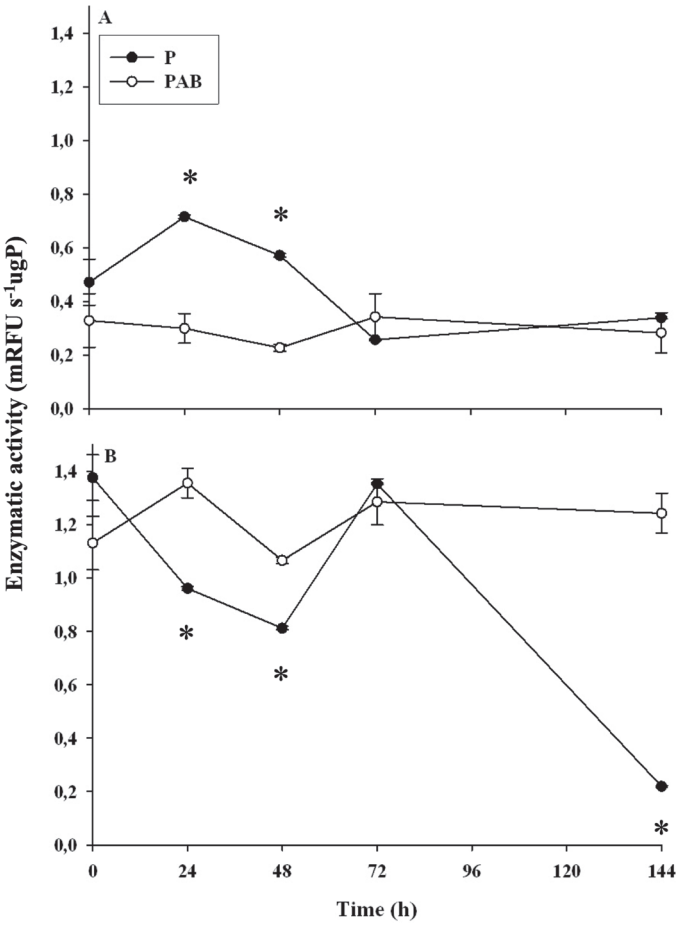

Fig. 7. DEVDase (A) and WEHDase (B) enzymatic activities in *D. tertiolecta* cells with P (closed symbols) or PAB (open symbols) treatment. Results are shown as means ± SD of two replicates. Statistically significant differences ($P < 0.05$) between treatments are indicated by asterisks.

decreases (Neale *et al.*, 1993), producing an excess of reactive oxygen species. The slight decline in F_v/F_m in P-treated cultures in the long term could be attributed to senescence, which was corroborated by morphological analysis showing that chromatin marginalization started after 72 h (Fig. 3). As observed in plants, cell cultures and unicellular photosynthetic organisms, chromatin condensation has been found to accompany cell death after different types of induction mechanisms (Moharikar *et al.*, 2006; Darehshouri *et al.*, 2008; Jiménez *et al.*, 2009). This was the only effect observed in P-treated cells, as the rest of the organelles remained intact. PAB exposure produced a decrease in the growth rate and carrying capacity of the cultures compared with P-treated cultures (Fig. 1A) because DNA damage arrests the cell cycle (discussed below). For instance, phytoplankton growth rates are inhibited by UVR, and this was found to be five times higher in UVR-excluded treatments (Llabrés and Agustí, 2010).

The unavoidable consequence of these events in cell fate is death. It is well known that, despite protective systems and repair pathways, cell death is caused by UVR exposure in phytoplanktonic organisms, as demonstrated for natural phytoplankton populations from the Atlantic Ocean (Llabrés and Agustí 2006), and in controlled culture conditions in *Chlamydomonas* (Moharikar *et al.*, 2006) and *Dunaliella* (Jiménez *et al.*, 2009). However, cell death was not detected in any of the *D. tertiolecta* cultures stressed with UVR (Fig. 1, insert), indicating that this particular species is capable of tolerating UVR for at least 6 days. The most remarkable changes observed were the rapid disaggregation of the chromatin under PAB treatment after the first hours of exposure, while other cellular structures remained unchanged after 48 h, when only apparent degradation of the chloroplast began (Fig. 3). Hence, the nucleus suffered the effects of UVR stress in the short term, while the rest of the cell suffered it in the long term, indicating high cellular resistance. These results agreed with those obtained by flow cytometry. The cytograms showed that, with the UVR treatment, the number of cells in G1 decreased exponentially due to rapid disaggregation of the chromatin (Fig. 2); therefore, the cell cycle could not be assessed. This was a direct consequence of UVR confirmed by other studies in which UVB exposure induced doubling of the cell volume in *Dunaliella salina*, a phenomenon that has been attributed to DNA damage and consequent cessation of the processes involved in the cell cycle (Masi and Melis, 1997). The same effect has been observed in other algae exposed to UVB (Behrenfeld *et al.*, 1992) and has been attributed to direct damage to the microtubules, resulting in a slow down of the G2 phase (Zaremba *et al.*, 1984; Staxen *et al.*, 1993). In our experiments, cell-cycle arrest by DNA damage was confirmed by the detection and accumulation of CPDs (Fig. 4).

Regarding the optimal quantum yield data, it was obvious that cells were photosynthetically active. This explains the high accumulation of starch that was observed (Fig. 3, see PAB panel at 24 h). The energy produced by photosynthesis is not demanded by cell division, because the cell cycle is arrested due to DNA damage and the energy is stored as starch. It is known that plant abiotic stress affects metabolism kinetics, resulting in the accumulation of starch (Muñoz *et al.*, 2006). This accumulated energy could be advantageous for the cell if the cause of the stress disappears.

The results showed a decrease in F_v/F_m and growth rates in PAB-treated cultures at the end of the experiment (Fig. 1) due to the accumulation of DNA damage caused by UVR, which results in the continuous inhibition of the synthesis of numerous proteins. This has a direct consequence on cell replication, photosynthesis, and other essential processes, but it did not produce cell death, as demonstrated by the absence of green fluorescent labelling in all treatments (Fig. 1, insert).

DNA damage and repair mechanisms triggered by UVR

DNA is a principal target of shortwave radiation in algae. DNA predominantly absorbs in the UVB region, largely contributing to lethal damage (reviewed by Buma *et al.*, 2003). Formation of CPDs is the most common injury associated with UVB exposure, causing the disruption of DNA replication (Buma *et al.*, 2001; Helbling *et al.*, 2001). In contrast, exposure to UVA has different effects on DNA, most of them indirectly through the formation of reactive oxygen species and the production of modified bases (Jeffrey and Mitchell, 1997). However, UVA has a relevant role in the removal of CPDs through a photoreactivation mechanism

that eliminates UVR-induced photoproducts through the action of a photolyase, an enzyme that uses the energy of UVR or PAR to break the dimers, restoring the DNA integrity (Britt, 2004). Our results showed that PAB treatment induced CPD formation after just 8 h of exposure (data not shown), reaching an accumulation level ten times higher at the end of the experiments than at the beginning. In contrast, P-treated cultures, as expected, showed no increase in the amount of CPDs during the 6 days of exposure (Fig. 4). However, the damage caused by PAB treatment did not completely suppress DNA replication. Studies in macrophytes have shown that species such as *Palmaria palmata*, *Devaleraea ramentacea*, *Phycodrys rubens*, and *Laminaria saccharina* have the capacity to remove 90% of induced CPDs in just 5 h, although other species such as *Odonthalia dentata*, *Coccotylus truncates*, and *Monostroma arcticum* did not show this capacity (Van de Poll *et al.*, 2002). These studies concluded that CPD induction is lower in the Arctic than in temperate and tropical regions. This low capacity of arctic macrophytes seemed to be enough to prevent accumulation of CPDs in their natural habitat. Boelen et al. (2001) observed these same repair mechanisms in tropical phytoplankton when the UVR dose was reduced, and also during and after exposure to UVR of bacteria and phytoplankton in the Red Sea (Boelen *et al.*, 2002). Nevertheless, these mechanisms were not sufficient to remove DNA damage, suggesting that photomortality is responsible for the loss of the plankton community, which was not the same in our case.

Cell density increased slightly during UVR exposure, so it could be concluded that there are mechanisms for CPD removal, probably by activation of photolyases through UVA, as well as other repair mechanisms induced by the detection of DNA damage. Among these, NER and BER are the most important. BER is a critical pathway in cellular defence against endogenous or exogenous DNA damage. This complex multistep process is initiated by DNA glycosylases that excise the damaged base and continues through the concerted action of additional proteins that finally restore the DNA to the unmodified state (Fortini and Dogliotti, 2007). BER has been studied in detail in eukaryotes, and Córdoba-Cañero *et al*. (2009) extended the biochemical analysis to plants, demonstrating that *Arabidopsis* cell extracts were able to fully repair U:G mismatches initiated by glycosylase activity. In vascular plants, active DNA demethylation is carried out mainly by a small group of bifunctional DNA glycosylases, including ROS1, DME, DML2, and DML3 [founding members of the DEMETER-LIKE (DML) family]. Once these DNA glycosylases remove the methylated cytosine base and create an abasic site, the gap is refilled with an unmethylated cytosine through a BER pathway (Zhu, 2009). Accordingly, our results showed an accumulation of a ROS1-like protein in response to UVR treatment from 48 h of exposure to the end of the experiment (Fig. 5B). A positive correlation was found between TT dimmers and ROS1 accumulation ($P < 0.0001$, $r = 0.766$). In *A. thaliana*, the molecular weight for ROS1 is around 160 kDa, but it has been demonstrated that members of the DML family are large polypeptides that possess a discontinuous catalytic domain (Ponferrada-Marín *et al.*, 2010). The antibody we used was raised against a 30 kDa peptide, which is the specific part of the AtROS1 protein. We obtained a single 52 kDa band that disappeared when the antibody was blocked with the recombinant protein, and that passed through all the non-specific binding tests performed (see Materials and Methods). Thus, we assumed that, in *D. tertiolecta*, the protein is smaller. In contrast, cultures without UVR exposure presented a basal amount of ROS1 throughout the experiment, without any significant change (Fig. 5B). This confirmed all the previous results with regard to cell-cycle progress, morphology, and CPD accumulation, and it also confirmed all the triggered repair mechanisms such as BER and NER, which allowed the cells to survive under UVR. This hypothesis was corroborated by PCNA accumulation, another protein involved in DNA repair. PCNA has received considerable attention because of its role in multiple cellular pathways. In addition to DNA replication and repair events such as base excision, it is also involved in various other processes including NER (Nichols and Sancar, 1992), mismatch repair (Umar *et al.*, 1996), cell-cycle control (Watanabe *et al.*, 1998), apoptosis (Scott *et al.*, 2001), and transcription (Hasan *et al.*, 2001). The primary amino acid sequences of PCNA are highly conserved across the eukaryotic kingdom and more than 90% homology has been observed among plant PCNA proteins (Bagewadi *et al.*, 2004).

In our experiments, it was shown that damage caused to the DNA triggers the accumulation of this protein from the start of the PAB treatment (Fig. 5A). As exposure under UVR was extended, the synthesis of PCNA was higher because accumulation of damage was greater, as shown by the CPD results. A positive correlation was found between TT dimmers and PCNA accumulation ($P < 0.0001$, $r = 0.893$). These data agree with changes in cell morphology, as detected by disaggregation of chromatin within hours after the outset of the treatment. The basal amount of protein found at the beginning of the experiments is appointed to cell division, because PCNA is also involved in DNA replication (Carpenter *et al.*, 1998), since it is a polymerase auxiliary protein and its presence in the nucleus of *D. tertiolecta* indicates that cells are in S phase of the cell cycle (Lin *et al.*, 1995). A positive correlation was found between ROS1 and PCNA accumulation ($P < 0.0001$, $r = 0.790$).

MAPK phosphorylation and the response to stress

The presence and phosphorylation of three MAPK-like proteins was detected in *D. tertiolecta* in response to UVR (Fig. 6). These MAPK-like proteins were most similar to mammalian p38, JNK, and ERK1/2, and showed different behaviours depending on the presence or not of UVR. Six MAPK cascades have been proposed to date in mammalian cells, in only three of which (p38, c-Jun, and ERK) all components have been completely identified. These cascades are involved in the response to a variety of stress conditions (UVR, heat, osmolarity, growth factors, hormones, etc.) and control of cell proliferation and differentiation. In previous studies, we demonstrated that p38-like and JNK-like MAPKs were responsible for stress adaptation in *D. viridis*, while ERK1/2-like protein was involved in cell division control (Jiménez *et al.*, 2004, 2007). In the current study, it was found that increased phosphorylation of a 40 kDa p38-like MAPK occurred in *D. tertiolecta* in the first 24 h after exposure to UVR, and the degree of phosphorylation was progressively reduced to initial levels by 144 h (Fig. 6B). However, activation of this protein with P treatment was much lower and occurred

progressively during the first 72 h of exposure. JNK-like MAPK was also activated with both in P and PAB treatment, but, activation was higher in the latter and the course of the activation was more extended over time (Fig. 6A). Finally, an ERK-like MAPK was also highly phosphorylated with P treatment during the first days (Fig. 6C), in parallel with the exponential phase of division of *D. tertiolecta*. These results indicated a relationship between UVR stress and p38 and JNK phosphorylation, and, as expected, a decrease in ERK phosphorylation in stressed cells. Jiménez *et al*. (2007) showed that ERK phosphorylation was mandatory for completing cell division in *D. viridis*, and that several environmental stresses resulted in cell division reduction or arrest due to ERK dephosphorylation.

Both p38 and JNK have been extensively described to be responsible for stress adaptation in animal cells (Capasso *et al.*, 2001). Among these stresses, it is worth mentioning hyperosmolarity and UVR exposure. With regard to *D. tertiolecta*, a similar response was obtained, with a significant increase in the phosphorylation of both kinases in response to UVR stress. We have shown previously that inhibition of p38 and JNK phosphorylation in *D. viridis* highly impaired adaptation under stressful conditions, as was the case with *D. tertiolecta*. These results indicate that this microalga survives under high UVR stress conditions by activating several cell programmes, among them p38- and JNK-like MAPKs and DNA repair mechanisms such as PCNA plus ROS1 accumulation and CL activities.

CL activities as stress proteins

Caspase-like activities have been reported to be involved in PCD in organisms other than metazoans (Segovia *et al.*, 2003; Deponte, 2008; Bouchard and Purdie, 2011). However, execution of PCD in non-metazoan organisms is morphologically different from apoptotic PCD in animals; it lacks a number of key molecular components of the apoptotic machinery and in some cases might be referred to as 'apoptotic-like'. With regard to phytoplankton, the nature of CL activities currently remains an unravelled question. There are no orthologue caspase genes reported to date in kingdoms other than that of metazoans, and metacaspases, which are distant homologues of caspases within the cysteine protease superfamily, found in fungi, vascular plants, and unicellular eukaryotes, were thought to perform similar functions to caspases. However, their target substrates are quite distinct. In the majority of cases, measurement of these activities in unicellular species has been carried out using the classical aspartate-containing caspase substrates. Consequently, the activities measured are 'CL' activities and not metacaspases, as metacaspase activity has not yet been reported in phytoplankton (metacaspases are calcium-activated enzymes having target sites in P1 lysine or arginine; reviewed by Tsiatsiani *et al.*, 2011).

Therefore, the question is: which enzyme is responsible for the observed CL activity in phytoplankton (as well as in plants, fungi, etc.)? Some authors have pointed to the serine protease family proteins to perform this hydrolysis in vascular plants (Bonneau *et al.*, 2008) and/or the vacuolar processing enzyme (Hara-Nishimura and Hatsugai, 2011). It has also been reported that some CL activities are attributable to the plant subtilisin-like proteases—saspases and phytaspases. These proteases hydrolyse a range of tetrapeptide caspase substrates following the aspartate residue. Data obtained with saspases implicate them in the proteolytic degradation of Rubisco during biotic and abiotic PCD, whereas phytaspase-overproducing and silenced transgenics provide evidence that phytaspase regulates PCD during both abiotic (oxidative and osmotic stresses) and biotic (virus infection) insults. Like putative caspases, phytaspases and saspases are synthesized as pro-enzymes, which are processed autocatalytically to generate a mature enzyme. However, unlike caspases, phytaspases and saspases appear to be constitutively processed and secreted from healthy plant cells into the intercellular space (Vartapetian *et al.*, 2011), showing that there is specificity for aspartate residues and that traditional caspase inhibitors inhibit the above-mentioned proteinases. Even so, the discussion about whether metacaspases are caspases or not remains open (Carmona-Gutierrez *et al.*, 2010; Enoksson and Salvesen, 2010).

In any case, it is clear that further research is needed in phytoplankton and protists to unravel the nature of these proteases, which cleave after an aspartate residue in general. The fact is that they are present and show a 'preference' for this amino acid. However, although it is known that CL activities are involved in cell death in these organisms, these enzymes are also essential during the normal physiology of the cells, involved in housekeeping functions, as well as during growth and cell stress acclimation (Segovia and Berges 2005, Bouchard and Purdie 2011; Franklin *et al.*, 2012). Our results demonstrated that DEVDase and WEHDase enzymatic activities (Fig. 7) were present and active, showing a broad range of activity depending on the treatment, even though the cells were not dead, and so they must be involved during the response to stress. The proteolytic activity may then possibly be related to a shift to the arrested state, which is a low metabolic state but retains low photosynthetic levels as indicated by Fv/Fm, in this case due to repair responses that are able to keep the cell alive, viable, and accumulating starch to be used when the stress ceases. In this regard, a non-apoptotic-like role for CLs was proposed previously in phytoplankton. They were reported to be constitutive and to have housekeeping functions when *D. tertiolecta* cells were treated with several antibiotics that inhibited *de novo* protein synthesis (Segovia and Berges, 2005), and measurements of the enzymatic activities of 'XXXDase' demonstrated that they were active. Thus, growing evidence suggests the participation of CLs in other cellular processes such as development, the cell cycle, and cell proliferation, in addition to their well-characterized role in cell death. We have provided evidence that these CL proteases must be considered within a wider general meaning of stress proteins, rather than specifically being involved in cell death in phytoplankton.

UVR as a selection pressure factor for phytoplankton

Phytoplankton is at the base of the trophic web and is an important component of biogeochemical cycles; thus, research on the ecophysiology of phytoplankton is of relevance. On our planet, half of the organic carbon incorporation is due to phytoplankton (Raven, 2011) and evaluation of UVR effects on aquatic

ecosystems is crucial to estimate carbon flux in the oceans and increase our understanding of global change (Sarmiento et al., 2004). The stress caused by UV solar radiation depends on various factors. The first is that the radiation levels on the mixed layer must be high enough to produce CPDs and photoinhibition. It is through these first few metres of the water column where UVR is able to penetrate, depending on the transparency of the water, hence causing damage. The second factor is the ability of cells to repair the damage. Our data showed the capacity of *D. tertiolecta* to undergo DNA repair. This species can tolerate high doses of UVR for several days, despite damage caused to DNA and essential proteins. Similar data were obtained by Montero et al. (2002) in a study comparing the optimum quantum yield of seven species of microalgae from different phyla subjected to UVR treatments, in which *D. salina* was the most UV-tolerant among the Chlorophyta.

The explanation for the high resilience of this species can be found in the sequence of temporal events taking place during UVR stress. Biochemical responses precede any structural change or modification. In this regard, we saw that the F_v/F_m value dropped off in matter of 2 h as a result of photosynthetic uncoupling because of photoinhibition within the frame of 'short-term responses'. Concurrently, the DNA was also modified by the formation of CPDs during the short-term response. As a consequence of the UVR-induced biochemical changes, MAPKs were activated by dual phosphorylation, initiating downstream repair processes through PCNA and ROS1 accumulation. In this mid-term time frame, CL activities (which should be expected to help in dismantling the cell according to the traditional role in cell death usually attributed to these enzymes in a variety of organisms) were not related to cell death processes, indicating a role in overcoming/managing the stress. All the biochemical changes that happened during the short- and mid-term response induced structural modifications affecting the cell cycle and morphology.

Our results suggest that the repair capacity of *D. tertiolecta* and the consequent tolerance to high UVR doses could provide a clear advantage over other phytoplankton species in the photic zone and possibly in the whole water column. Moreover, although projections on the dynamics of the ozone holes indicate changes in distribution, geography, and size (Shanklin, 2010), the capability of *D. tertiolecta* to repair UV-induced damage to DNA and essential proteins would confer clear advantages to this species with regard to dominance and exclusions. The high resilience to abiotic stress of some species such as small chlorophytes could be crucial for phytoplankton vertical community structure and biogeography within the actual global-change scenario.

Acknowledgements

This work was supported by research grants P08-03800 from the Regional Science Research Programme (Junta de Andalucía, Spain) and CTM/MAR 2010-17216 from the Ministry for Science and Innovation (MICCIN) Spain, to M.S., and CTM/ANT 2011-24007 to C.J. The authors are truly grateful to Teresa Roldán-Arjona (Córdoba University, Spain) for providing us with the AtROS1 antibodies, the recombinant proteins used as antigens and the pre-immune sera.

References

Bagewadi B, Chen S, Lal SK, Roy Choudhury N, Mukherjee SK. 2004. PCNA interacts with Indian mung bean yellow mosaic virus Rep and downregulates Rep activity. *Virology Journal* **78,** 11890–11903.

Behrenfeld MJ, Ardí JT, Lee H. 1992. Chronic effects of UVB on growth and cell volume of *Phaeodactilum tricornutum* (Bacillariophycea). *Journal of Phycology* **28,** 757–760.

Ben-Amotz A, Polle JEW, Rao DVS. 2009. *The Alga Dunaliella: Biodiversity, Physiology, Genomics, and Biotechnology*. Enfield, New Hampshire: Science Publishers.

Bidle KD, Haramaty L, Barcelo e Ramos J, Falkowski PG. 2007. Viral activation and recruitment of metacaspases in the unicellular coccolithophore, *Emiliania huxleyi*. *Proceedings of the National Academy of Sciences, USA* **104,** 6049–6054.

Boelen P, Obernosterer I, Vink AA, Buma AGJ. 1999. Attenuation of biologically affective UV radiation in tropical Atlantic waters, as measured with a biochemical DNA dosimeter. *Photochemistry and Photobiology* **69,** 34–40.

Boelen P, Post AF, Veldhuis MJW, Buma AGJ. 2002. Diel patterns of UVBR-induced DNA damage in picoplankton size fractions from the Gulf of Aqaba, Red Sea. *Microbial Ecology* **44,** 164–174.

Boelen P, Veldhuis MJW, Buma AGJ. 2001. Accumulation and removal of UVBR-induced DNA damage in marine tropical plankton subjected to mixed and simulated non-mixed conditions. *Aquatic Microbial Ecology* **24,** 265–274.

Bonneau L, Ge Y, Drury GE, Gallois P. 2008. What happened to plant caspases? *Journal of Experimental Botany* **59,** 491–499.

Bouchard JN, Campell DA, Roy S. 2005. Effects of UV-B radiation on the D1 protein repair cycle of natural phytoplankton communities from three latitudes (Canada, Brazil, and Argentina). *Journal of Phycology* **41,** 273–286.

Bouchard JN, Purdie DA. 2011. Temporal variation of caspase 3-like protein activity in cultures of the harmful dinoflagellates *Karenia brevis* and *Karenia mikimotoi*. *Journal of Plankton Research* **33,** 961–972.

Britt AB. 2004. Repair of DNA damage induced by solar UV. *Photosynthesis Research* **81,** 105–112.

Buma AGJ, Boelen P, Jeffrey WA. 2003. UVR-induced DNA damage in aquatic organisms. In: Helbling EW and Zagarese H, eds. *UV effects in aquatic organisms and ecosystems*. Comprehensive Series in Photochemical and Photobiological Sciences, Royal Society of Chemistry, 291–327.

Buma AGJ, Helbling EW, de Boer MK, Villafañe VE. 2001. Patterns of DNA damage and photoinhibition in temperate South-Atlantic picophytoplankton exposed to solar ultraviolet radiation. *Journal Photochemistry and Photobiology* **62,** 9–18.

Capasso JM, Rivard CJ, Berl T. 2001. The expression of the G subunit of Na, K-ATPase is regulated by osmolality and by C-terminal Jun kinase and PI3 kinase dependent mechanisms. *Proceedings of the National Academy of Sciences, USA* **98,** 13414–13419.

Carmona-Gutierrez D, Fröhlich KU, Kroemer G, Madeo F. 2010. Metacaspases are caspases. Doubt no more. *Cell Death and Differentiation* **17,** 377–378.

Carpenter EJ, Lin S, Chang J. 1998**.** Phytoplankton growth studies by cell cycle analysis. In: Cooksey KE, ed. *Molecular approaches to the study of the ocean*. London: Chapman & Hall, 227–245.

Córdoba-Cañero D, Morales-Ruiz T, Roldán-Arjona T, Ariza RR. 2009. Single-nucleotide and long-patch base excision repair of DNA damage in plants. *The Plant Journal* **60,** 716–728.

Darehshouri A, Affenzeller M, Lutz-Meindl U. 2008. Cell death upon H2O2 induction in the unicellular green alga *Micrasterias*. *Plant Biology* **10,** 732–745.

Deponte M. 2008. Programmed cell death in protists. *Biochimica et Biophysica Acta Molecular Cell Research* **1783,** 1396–1405.

Enoksson M, Salvesen GS. 2010. Metacaspases are not caspases – always doubt. *Cell Death and Differentiation* **17,** 1221.

Fortini P, Dogliotti E. 2007. Base damage and single-strand break repair: mechanisms and functional significance of short- and long-patch repair subpathways. *DNA Repair* **6,** 398–409.

Franklin DJ, Airs RL, Fernandes M, Bell TG, Bongaerts RJ, Berges JA, Malin G. 2012. Identification of senescence and death in *Emiliania huxleyi* and *Thalassiosira pseudonana*: cell staining, chlorophyll alterations, and dimethylsulfoniopropionate (DMSP) metabolism. *Limnology and Oceanography* **57,** 305–317.

García-Ortiz M-V, Ariza RR, Roldán-Arjona T. 2001. A chemiluminescent method for the detection of DNA glycosylase/lyase activity. *Analytical Biochemistry* **298,** 127–129.

Genty B, Briantais JM, Baker NR. 1989. The relationship between the quantum yield of photosynthetic electron-transport and quenching of chlorophyll fluorescence. *Biochimica et Biophysica Acta* **990,** 87–92.

Goldman JC, McCarthy JJ. 1978. Steady state growth and ammonium uptake of a fast growing marine diatom. *Limnology and Oceanography* **23,** 695–703.

Gong Z, MoralesRuiz T, Ariza RR, RoldánArjona T, David L. Zhu JK. 2002. ROS1, a repressor of transcriptional gene silencing in *Arabidopsis*, encodes a DNA glycosylase/lyase. *Cell* **111,** 803–814.

Guillard RRL, Ryther JH. 1962. Studies of marine planktonic diatoms. I. *Cyclotella nana* Hustedt and *Detonula confervacea* (Cleve) Gran. *Canadian Journal of Microbiology* **8,** 229–239.

Häder DP, Kumar HD, Smith RC, Worrest RC. 2007. Effects of solar UV radiation on aquatic ecosystems and interactions with climate change. *Photochemical & Photobiological Sciences* **6,** 267–285.

Hanelt D. 1998. Capability of dynamic photoinhibition in Artic macroalgae is related to their depth distribution. *Marine Biology* **131,** 361–369.

Hara-Nishimura I, Hatsugai N. 2011. The role of vacuole in plant cell death. *Cell Death and Differentiation* **18,** 1298–1304.

Hasan S, Hassa PO, Imhof R, Hottiger MO. 2001. Transcription coactivator p300 binds PCNA and may have a role in DNA repair synthesis. *Nature* **410,** 387–391.

Helbling EW, Buma AGJ, Boer MK, Villafañe VE. 2001. In situ impact of solar ultraviolet radiation on photosynthesis and DNA in temperate marine phytoplankton. *Marine Ecology Progress Series* **211,** 43–49.

Jeffrey WH, Mitchell DL. 1997. Mechanisms of UV-induced DNA damage and response in marine microorganisms. *Photochemistry and Photobiology* **65,** 260–263.

Jiménez C, Berl T, Rivard CJ, Edelstein CL, Capasso JM. 2004. Phosphorylation of MAP kinase-like proteins mediate the response of the halotolerant alga *Dunaliella viridis* to hypertonic shock. *Biochimica et Biophysica Acta* **1644,** 61–69.

Jiménez C, Capasso JM, Edelstein CL, Rivard CJ, Lucia S, Breusegem S, Berl T, Segovia M. 2009. Different ways to die: cell death modes of the unicellular chlorophyte *Dunaliella viridis* exposed to various environmental stresses are mediated by the caspase-like activity DEVDase. *Journal of Experimental Botany* **60,** 815–828.

Jiménez C, Cossío BR, Rivard CJ, Berl T, Edelstein CL, Capasso JM. 2007. Cell division in the unicellular microalga *Dunaliella viridis* depends on phosphorylation of extracellular signal-regulated kinases (ERKs). *Journal of Experimental Botany* **58,** 1001–1011.

Jordan BR. 1996. The effects of ultraviolet-B radiation on plants: a molecular perspective. *Advances in Botanical Research* **22,** 97–162.

Krokan HE, Standal R, Slupphaug G. 1997. DNA glycosylases in the base excision repair of DNA. *Biochemistry Journal* **325,** 1–16.

Kyriakis JM, Avruch J. 2001. Mammalian mitogen-activated protein kinase signal transduction pathways activated by stress and inflammation. *Physiology Review* **81,** 807–869.

Lesser MP. 2006. Oxidative stress in marine environments: biochemistry and physiological ecology. *Annual Review of Physiology* **68,** 253–278.

Lin S, Chang J. Carpenter EJ. 1995. Growth characteristic of phytoplankton determined by cell cycle proteins: PCNA immunostaining of *Dunaliella tertiolecta*. *Journal of Phycology* **31,** 388–395.

Llabrés M, Agustí S. 2006. Picophytoplankton cell death induced by UV radiation: evidence for oceanic Atlantic communities. *Limnology and Oceanography* **51,** 21–29.

Llabrés M, Agustí S. 2010. Effects of ultraviolet radiation on growth, cell death and the standing stock of Antarctic phytoplankton. *Aquatic Microbial Ecology* **59,** 151–160.

Lo HL, Nakajima S, Ma L, Walter B, Yasui B, Ethell DW, Owen LB. 2005. Differential biologic effects of CPD and 6-4PP UV-induced DNA damage on the induction of apoptosis and cell-cycle arrest. *BMC Cancer* **5,** 135.

Masi A, Melis A. 1997. Morphological and molecular changes in the unicellular green algae *Dunaliella salina* grown under supplemental UVB radiation: cell characteristic and photosystem II damages and repair properties. *Biochimica et Biophysica Acta* **1321,** 183–193.

Masih PJ, Kunnev D, Melendy T. 2008. Mismatch repair proteins are recruited to replicating DNA through interaction with proliferating cell nuclear antigen (PCNA). *Nucleic Acids Research* **36,** 67.

Meador JA, Baldwin AJ, Catala P, Jeffrey WH, Joux F, Moss JA, Pakulski JD, Stevens R, Mitchell DL. 2009. Sunlight-induced DNA damage in marine micro-organisms collected along a latitudinal gradient from 70°N to 68°S. *Photochemistry and Photobiology* **85,** 412–420.

Melis A, Nemson JA, Harrison MA. 1992. Damage to functional components and partial degradation of photosystem-II reaction center proteins upon chloroplast exposure to ultraviolet-B radiation. *Biochimica et Biophysica Acta* **1100,** 312–320.

Moharikar S, D'Souza JS, Kulkarni AB, Rao BJ. 2006. Apoptotic-like cell death pathway is induced in unicellular chlorophyte *Chlamydomonas reinhardtii* (Chlorophyceae) cells following UV irradiation: detection and functional analyses. *Journal of Phycology* **42,** 423–433.

Montero O, Klisch M, Häder DP, Lubian LM. 2002. Comparative sensitivity of seven marine microalgae to cumulative exposure to UVB radiation with daily increasing doses. *Botanica Marina* **45,** 305–315.

Morales-Ruiz T, Ortega-Galisteo AP, Ponferrada-Marín MI, Martínez-Macías MI, Ariza RR, Roldán-Arjona T. 2006. DEMETER and REPRESSOR OF SILENCING 1 encode 5-methylcytosine DNA glycosylases. *Proceedings of the National Academy of Sciences, USA* **103,** 6853–6858.

Muñoz FJ, Zorzano MTM, Alonso-Casajús N, Baroja-Fernández E, Etxeberria E, Pozueta-Romero J. 2006. New enzymes, new pathways and an alternative view on starch biosynthesis in both photosynthetic and heterotrophic tissues of plants. *Biocatalysis and Biotransformation* **24,** 63–76.

Nakagami H, Pitzschke A, Hirt H. 2005. Emerging MAP kinase pathways in plant stress signalling. *Trends in Plant Science* **10,** 339–346.

Neale PJ, Cullen JJ, Lesser MP, Melis A, Yamamoto H, Smith CM. 1993. Physiological bases for detecting and predicting photoinhibition of aquatic photosynthesis by PAR and UV radiation. In: Yamamoto HY, Smith CM (eds) *Photosynthetic Responses to the Environment Symposium*, 24–27 August 1992. Hawaii Institute of Tropical Agriculture and Human Resources, University of Hawaii. *American Society of Plant Physiology*, 61–77.

Nedelcu AM, Driscoll WW, Durand PM. Herron MD, Rashidi A. 2011. On the paradigm of altruistic suicide in the unicellular world. *Evolution* **65,** 3–20.

Nichols AF, Sancar A. 1992. Purification of PCNA as a nucleotide excision repair protein. *Nucleic Acids Research* **20,** 2441–2446.

Ortega-Galisteo AP, Morales-Ruiz T, Ariza RR, Roldán-Arjona T. 2008. *Arabidopsis* DEMETER-LIKE proteins DML2 and DML3 are required for appropriate distribution of DNA methylation marks. *Plant Molecular Biology* **67,** 671–681.

Parages ML, Capasso JM, Meco V, Jiménez C. 2012. A novel method for phosphoprotein extraction from macroalgae. *Botanica Marina* **55, doi 10.1515/bot-2011-0051 (in press).**

Pérez-Martín JM. 2008. *Programed cell death in protozoa*. Austin, TX: Landes Bioscience.

Ponferrada-Marín MI, Martínez-Macías MI, Morales-Ruiz T, Roldán-Arjona T, Ariza RR. 2010. Methylation-independent DNA binding modulates specificity of repressor of silencing 1 (ROS1) and facilitates demethylation in long substrates. *Journal of Biological Chemistry* **285,** 23032–23039.

Raven JA. 2011. The cost of photoinhibition. *Physiologia Plantarum* **142,** 87–104.

Roldán-Arjona T, Ariza RR. 2009. Repair and tolerance of oxidative DNA damage in plants. *Mutation Research* **681,** 169–179.

Roldán-Arjona T, García-Ortiz M-V, Ruiz-Rubio M, Ariza RR. 2000. cDNA cloning, expression and functional characterization of an *Arabidopsis thaliana* homologue of the *Escherichia coli* DNA repair enzyme endonuclease III. *Plant Molecular Biology* **44,** 43–52.

Ross CR, Paul VJ. 2006. Signal transduction in the cyanobacteria *Lyngbya confervoides* and *L. polychroa*: ecological implications of reactive oxygen species. *Integrative and Comparative Biology* **46,** E121.

Sarmiento JL, Slater R, Barber R, *et al.*. 2004. Response of ocean ecosystems to climate warming. *Global Biogeochemical Cycles* **18,** GB3003.

Scharer OD, Jiricny J. 2001. Recent progress in the biology, chemistry and structural biology of DNA glycosylases. *Bioessays* **23,** 270–281.

Schreiber U, Schilwa U, Bilger W. 1986. Continuous recording of photochemical and non-photochemical chlorophyll fluorescence quenching with a new type of modulation fluorometer. *Photosynthesis Research* **10,** 51–62.

Scott M, Bonnefin P, Vieyra D, Boisvert FM, Young D, Bazett-Jones DP, Riabowol K. 2001. UV-induced binding of ING1 to PCNA regulates the induction of apoptosis. *Journal Cell Science* **114,** 3455–3462.

Segovia M, Berges JA. 2005. Effect of inhibitors of protein synthesis and DNA replication on the induction of proteolytic activities, caspase-like activities and cell death in the unicellular chlorophyte *Dunaliella tertiolecta*. *European Journal of Phycology* **40,** 21–30.

Segovia M, Berges JA. 2009. Inhibition of caspase-like activities prevents the appearance of reactive oxygen species and dark-induced apoptosis in the unicellular chlorophyte *Dunaliella tertiolecta*. *Journal of Phycology* **40,** 21–30.

Segovia M, Haramaty L, Berges JA, Falkowski PG. 2003. Cell death in the unicellular chlorophyte *Dunaliella tertiolecta*: a hypothesis on the evolution of apoptosis in higher plants and metazoans. *Plant Physiology* **132,** 99–105.

Shanklin J. 2010. Reflections on the ozone hole. *Nature* **465,** 34–35.

Staxen I, Bergounioux C, Borman JF. 1993. Effects of UV on cell division and microtubule organisation in *Petunia hybrida* protoplasts. *Protoplasma* **173,** 70–76.

Timmermans KR, Veldhuis MJW, Brussaard CPD. 2007. Cell death in three marine diatom species in response to different irradiance levels, silicate, or iron concentrations. *Aquatic Microbial Ecology* **46,** 253–261.

Tsiatsiani L, Van Breusegem F, Gallois P, Zavialov A, Lam E, Bozhkov PV. 2011. Metacaspases. *Cell Death and Differentiation* **18,** 1279–1288.

Umar A, Buermeyer AB, Simon JA, Thomas DC, Clark AB, Liskay RM, Kunkel TA. 1996. Requirement for PCNA in DNA mismatch repair at a step preceding DNA resynthesis. *Cell* **87,** 65–73.

Van de Poll WH, Hanelt D, Hoyer K, Buma AGJ, Breeman AM. 2002. Ultraviolet-B-induced cyclobutane–pyrimidine dimer formation and repair in arctic marine macrophytes. *Photochemistry and Photobiology* **76,** 493–500.

Vardi A, Berman-Frank I, Rozenberg T, Hadas O, Kaplan A, Levine A. 1999. Programmed cell death of the dinoflagellate *Peridinium gatunense* is mediated by CO2 limitation and oxidative stress. *Current Biology* **9,** 1061–1064.

Vartapetian AB, Tuzhikov AI, Chichkova NV, Taliansky M, Wolpert TJ. 2011. A plant alternative to animal caspases: subtilisin-like proteases. *Cell Death and Differentiation* **18,** 1289–1297.

Veldhuis MJW, Kraay GW, Timmermans KR. 2001. Cell death in phytoplankton: correlation between changes in membrane permeability, photosynthetic activity, pigmentation and growth. *European Journal of Phycology* **36,** 167–177.

Watanabe H, Pan ZQ, Schreiber-Agus N, DePinho RA, Hurwitz J, Xiong Y. 1998. Suppression of cell transformation by the cyclin-dependent kinase inhibitor p57KIP2 requires binding to proliferating cell nuclear antigen. *Proceedings of the National Academy of Sciences, USA* **95,** 1392–1397.

Yi Y, Cao Y, Qian L, Min L, Long C, Lindan B, Zhirong Y, Dairong Q. 2006. Cloning and sequence analysis of the gene encoding (6-4) photolyase from *Dunaliella salina*. *Biotechnology Letters* **28,** 309–314.

Yoon JH, Lee CS, O'Connor TR, Yasui A, Pfeifer GP. 2000. The DNA damage spectrum produced by simulated sunlight. *Journal of Molecular Biology* **299,** 681–693.

Zaremba TG, LeBon TR, Millar DB, Smejkal RM, Hawley RJ. 1984. Effects of UV on the in vitro assembly of microtubules. *Biochemistry* **23,** 1073–1080.

Zhang T, Liu Y, Yang T, Zhang L, Xu S, Xue L, An L. 2006. Diverse signals converge at MAPK cascades in plant. *Plant Physiology Biochemistry* **44,** 274–283.

Zhu JK. 2009. Active DNA demethylation mediated by DNA glycosylases. *Annual Review of Genetics* **43,** 143–166.

Zuppini A, Gerotto C, Baldan B. 2010. Programmed cell death and adaptation: two different types of abiotic stress response in a unicellular chlorophyte. *Plant and Cell Physiology* **51,** 884–895.